Regular Article

PHYSICAL CHEMISTRY RESEARCH
Published by the
*Iranian Chemical Society*
www.physchemres.org
info@physchemres.org

***Phys. Chem. Res.**, Vol. 5, No. 4, 755-769, December 2017*
**DOI: 10.22036/pcr.2017.77577.1358**

# Theoretical Investigation of the Reaction Mechanism for a Type of N-heterocyclic Compound Involving Mono-N-aryl-3-aminodihydropyrrol

S.M. Habibi-Khorassani[a,*], M. Shahraki[a], S.Nouraei-Sarjou[a], M. Ansari-Fard[a] and A. Hatami[b]

[a]*Department of Chemistry, University of Sistan and Baluchestan, P. O. Box: 98135-674, Zahedan, Iran*
[b]*Department of Mathematics, University of Sistan and Baluchestan, P. O. Box: 98135-674, Zahedan, Iran*

*(Received 10 February 2017, Accepted 14 August 2017)*

The kinetics of reaction between 4-methylaniline (1), dimethyl acetylenedicarboxylate (2) and formaldehyde (4) has been theoretically investigated to gain further insight into the reaction mechanism. The results of theoretical calculations were achieved using the ab initio method at the HF/6-311G(d,p) level of theory in gas phase. The mechanism of this reaction had 5 steps. Theoretical kinetic data (k and $E_a$), activation parameters ($\Delta G^{\#}$, $\Delta S^{\#}$ and $\Delta H^{\#}$) and thermodynamic parameters ($\Delta G°$, ($\Delta S°$ and ($\Delta H°$) were calculated for each step and overall reaction. Step 2 of the mechanism was identified as the rate determining step. Also, the method of calculations was improved to B3LYP/6-311G(d,p) level of theory and the reaction mechanism was investigated for all steps of this reaction, again kinetic data and thermodynamic parameters were recalculated at this level of the theory. Improved data at this level was in a good agreement with the HF/6-311G(d,p) level of theory. Theoretical results, altogether were compatible with the literature's reports. As expected, $step_1$ and $step_3$ were recognized as the fast and fastest steps among the other steps. The overall reaction was enthalpy-controlled and proceeded chemically-controlled. In addition, $step_4$ was recognized relatively slow, because the five-membered ring formation in this step was inherently an energetically unfavorable process.

**Keywords:** N-heterocycles, Density functional theory, Aniline, Formaldehyde

## INTRODUCTION

A reaction in which three or more reactants are reacted together to produce a product in a single reaction vessel is a multi-component reaction [1,2]. Multi-component reaction is an ideal basic synthesis for some organic methodology such as convergence, atom and step economy, synthetic versatility, electivity, *etc.* [3-7]. Multi-component reactions (MCRs) especially with N-heterocycles products are becoming increasingly valuable in organic and medicinal chemistry [8]. N-heterocycles have various biological, medicinal and pharmaceutical applications, and in recent years the synthesis of these compounds have been found a considerable attention [8-10]. There are several bioactive natural molecules with a part of pyrrol-2-one [13,14] such as holomycin and thiolutin [14], thiomarinol A4 [15], oteromycin [16], pyrrocidine A [17], quinolactacinC [18], and ypaoamide [19]. In other words, dihydropyrrol-2-ones have been successfully used as peptidomimetic [20], HIV integrase [21], herbicidals [22], DNA polymerase inhibitors [23], caspase-3inhibitors [24] cytotoxicandantitumor agents [25], antibiotics [26] and also inhibitor softheannexin A2-S100A10 protein interaction [27]. Previously, kinetics of N-heterocycle compound and some organic reactants have been theoretically investigated [28-38]. A typical organic reaction proceeds using a special mechanism. There may be many proposed mechanisms for a typical organic reaction. Experimental methods have many instrumental limitations such as trapping the intermediates or transition states (TSs) in confirming the mechanism from which the reactions proceed. Computational methods can make confirming the mechanism easier, cheaper and more precise. Because the

*Corresponding author. E-mail: smhabibi@chem.usb.ac.ir

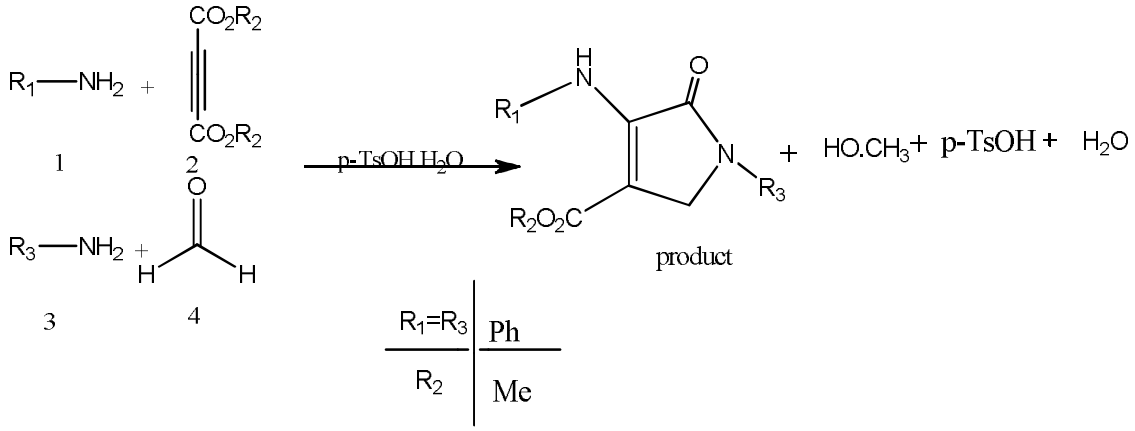


*Scheme 1.* The overall reaction between 1, 2, 3 and 4 compounds for the generation of mono-N-aryl-3-aminodihydropyrrol-2-one-4 carboxylate (product). $R_1$ and $R_3$ are the same in the present calculations

UV-Vis spectrophotometry method was not able to follow experimentally kinetics and the reaction mechanism of recent work, theoretical calculations were employed. The purpose of this study is to elucidate the mechanistic details related to the formation of mono-N-aryl-3-aminodi-hydropyrrol-2-one-4-carboxylate from the reaction between aniline (1), dimethyl acetylenedicarboxylate (2) and formaldehyde (4). Synthesis of the reaction has been previously reported [39].

## THEORETICAL SECTION

### Computational Methods

All geometries of the reactants (1, 2 and 3, 4), product, intermediates (5, 6, 7, 8), and transition states (TS1, TS2, TS3, TS4, TS5) involved in the reaction (Scheme 1) were optimized at the HF/6-311G(d,p) level of theory in the gas phase [40]. The stationary points were classified as true minima if there was no imaginary vibrational frequency. The transition states were characterized by the first imaginary vibrational frequency. The activation energies ($E_a$), the Arrhenius factors, and the rate constants were computed using Eqs. (1), (2) and (3), respectively on page 9, which were derived from the transition state theory [41]. All Calculation were performed with the Gaussian 09 program [42].

## RESULTS AND DISCUSSION

The reaction between dimethyl acetylenedicarboxylate (DMAD) 2, aniline 1 and formaldehyde 4 were performed in the presence of ρ-TsOH.$H_2O$ at room temperature for the generation of mono-N-aryl-3-aminodihydropyrrol-2-one-4-carboxylates as shown in Scheme 1.

Speculative reaction mechanism has been shown in Fig. 1 according to the literature's report [39]. How reliable is the proposed mechanism for the title reaction? (Fig. 1). This is the main question that we attempt to find an appropriate explanation by the following theoretical calculations.

The first step of the reaction starts with $C_2 \equiv C_3$ bond cleavage and N-$C_2$ bond formation (Fig. 2). In the stationary point (compound 2), the $C_1$-$C_2$, $C_2$-$C_3$ and $C_3$-$C_4$ bond lengths, $C_1$-$C_2 \equiv C_3$, $C_2 \equiv C_3$-$C_4$ bond angles and the dihedral angle of $C_1$-$C_2$-$C_3$-$C_4$ are 1.44, 1.2 and 1.45 Å, 135.44° and 121.568° and also 2.99°, respectively. The N and $C_2$ atoms are getting close, leading to the N-$C_2$ bond formation at intermediate 5($I_1$). The first transition state has a breaking $C_2$-$C_3$ bond distance of 1.32 Å , which is 0.12 Å longer than that in DMAD, and also forming N-$C_2$ bond distance of 1.47 Å. In the transition state ($TS_1$), the $C_1$-$C_2$, $C_2$=$C_3$ and $C_3$-$C_4$ bond lengths are 1.47, 1.32 and 1.43 Å, respectively. The $C_1$-$C_2$=$C_3$ and N…$C_2$=$C_3$ angles are 136.6° and 104.255°. Also, the $C_1$-$C_3$=$C_2$-$C_4$ dihedral angle is 2.94°. Corresponding bonds in the intermediate 5($I_1$), namely the

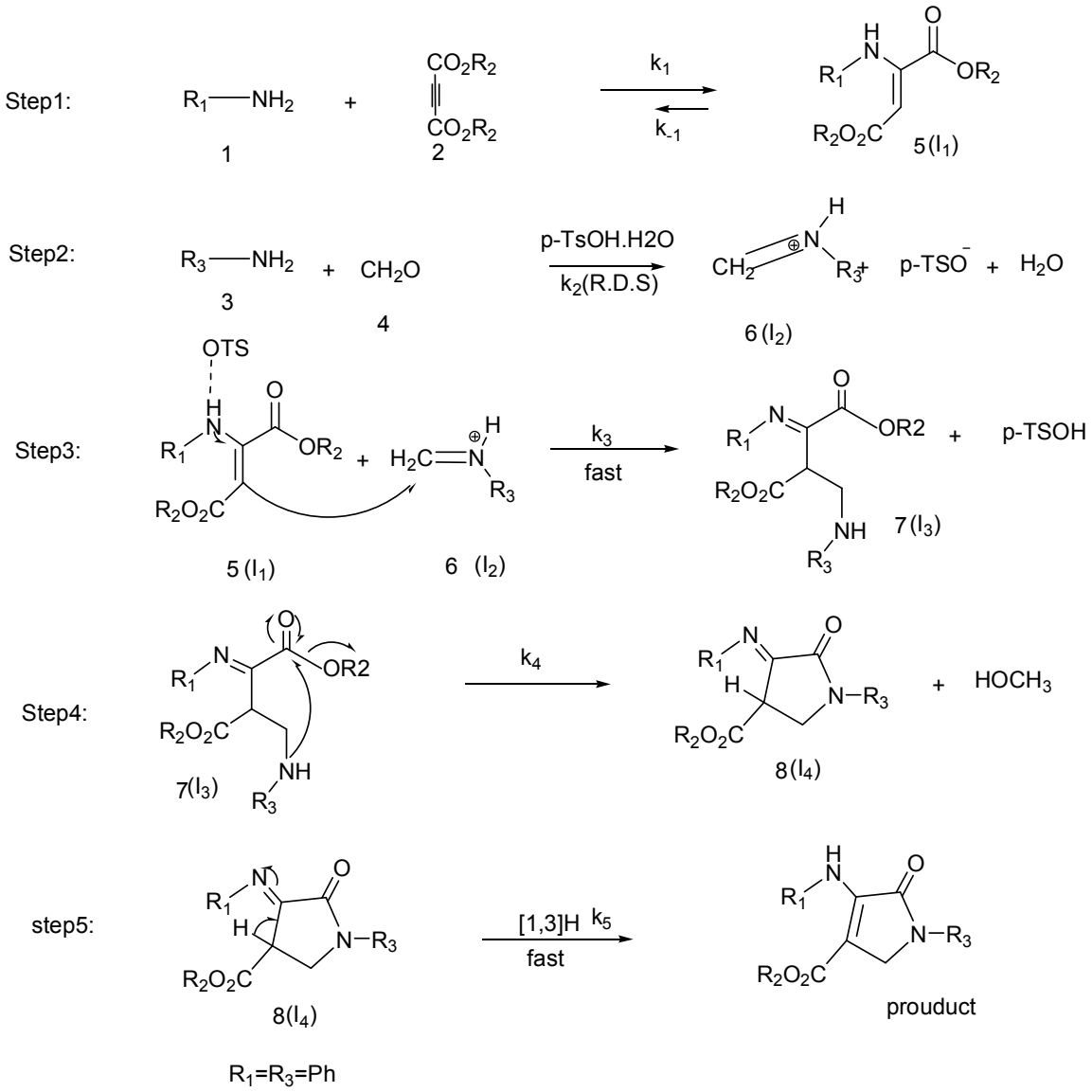


**Fig. 1.** The proposed mechanism between dimethyl acetylenedicarboxylate (DMAD) 2, aniline 1 and formaldehyde 4 in the presence of ρ-TsOH.$H_2O$ for the generation of mono-N-aryl-3-aminodihydropyrrol-2-one-4-carboxylate [39]. In this particular reaction, compounds 1 and 3 are the same.

$C_1$-$C_2$, $C_2$≡$C_3$ and $C_3$-$C_4$ bond lengths, are 1.50, 1.33 and 1.47 Å. The $C_1$-$C_2$=$C_3$ and N…$C_2$=$C_3$ angles are 124.95° and 125.89°, respectively. Also, the $C_1$-$C_2$=$C_3$-$C_4$ dihedral angle is 2.85°. These changes are summarized in Table 1.

As can be seen, three significant changes would be prospect:

1) $C_2$≡$C_3$ cleavage increase from compound 2 to intermediate 5

2) $C_1$-$C_2$ bond length increase in this order: intermediate 5 > $TS_1$ > compound 1+2

3) N-$C_2$≡$C_3$ angles take significant increasing from $TS_1$ to intermediate 5

For the generation of the $TS_1$ structure, it was required to proceed this procedure; the $N_{10}$ and $H_3$ atoms of aniline

**Table 1.** The Major Geometrical Parameters Containing Bond Lengths, Bond Angles and Dihedral Angles for Compounds 1+2, $TS_1$ and Intermediate 5($I_1$) in the First Step (Step 1) of Mechanism

| Species | Bond length (Å) | | | Bond angle (Degree) | | | Dihedral angle (Degree) |
|---|---|---|---|---|---|---|---|
| | $C_1$-$C_2$ | $C_2$≡$C_3$ | $C_3$-$C_4$ | $C_1$-$C_2$=$C_3$ | $C_2$≡$C_3$-$C_4$ | N-$C_3$≡C | $C_1$-$C_2$≡$C_3$-$C_4$ |
| Compound 1+2 | 1.44 | 1.2 | 1.45 | 135.44 | 121.568° | 116.001 | 2.99 |
| $Ts_1$ | 1.47 | 1.32 | 1.43 | 136.6° | 127.41 | 10 4.255 | 2.94 |
| Intermediate 5 | 1.5 | 1.33 | 1.47 | 124.95 | 126.49 | 125.89 | 2.85 |

As can be seen, three significant changes would be prospect: 1) $C_2$≡$C_3$ cleavage increase from compound 2 to intermediate 5; 2) $C_1$-$C_2$ bond length increase in this order: intermediate 5 > $TS_1$ > compound 1+2; 3) N-$C_2$≡$C_3$ angles take significant increasing from $TS_1$ to intermediate 5.

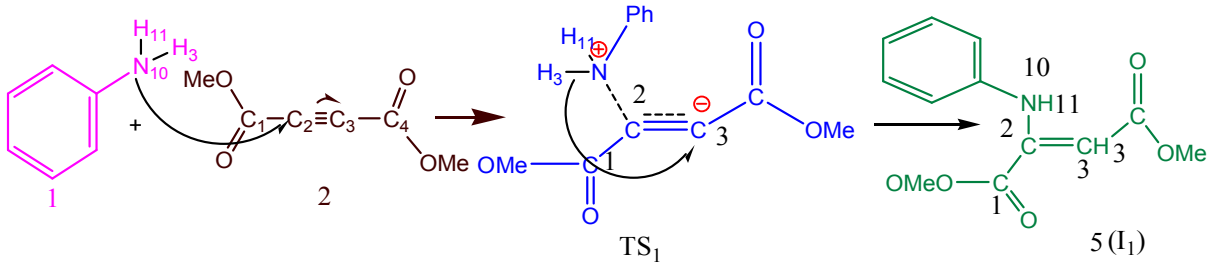


**Fig. 2.** Step$_1$ of the theoretical mechanism for the reaction between dimethyl acetylenedicarboxylate (DMAD) 2 and Aniline 1 for the generation of intermediate 5($I_1$).

compound should bind $C_2$ and $C_3$ atoms of DMAD 2, instantaneously. To do so, we put DMAD 2 and the aniline 1 structures in a far enough distance from each other, then in each step of scanning, $N_{10}$ is approaching to $C_2$ (in 0.1Å distance), through which $H_3$ is getting close to $C_3$ step by step until a peak is obtained (two dimensional scanning). After each scan, the result was represented in a diagram. This is the first generation of $TS_1$ when $N_{10}$ and $C_2$ atoms were kept in a constant distance.

Then, in the second scan, $N_{10}$ approaches to $C_2$ again (just in a 0.1 Å distance), at the same time, with respect to the new distance between $N_{10}$ and $C_2$ (second scan), $H_3$ is getting close to $C_3$ again step by step until a second peak of TS1 is generated. This behavior repeated for obtaining some other $TS_1$ (third, fourth, fifth and final scan) while in each scan, $N_{10}$ and $C_2$ atoms were kept in a new constant distance. These results are shown in a separate diagram in accordance with the energy of all TS points in each scan versus the changes in $N_{10}$-$C_2$ bond length, Fig. 4. Each point on this diagram is an exhibition of the possible TS for at least seven scans in this procedure (two dimensional scanning).

This diagram has a point with the lowest energy value that obtains the TS structure. The calculated stretching frequencies at HF/6-311G(d,p) and B3LYP/6-311G(d,p) levels, listed in Table 11, show that aniline, DMAD and intermediate 5($I_1$) are true minimum points. The $TS_1$ energy

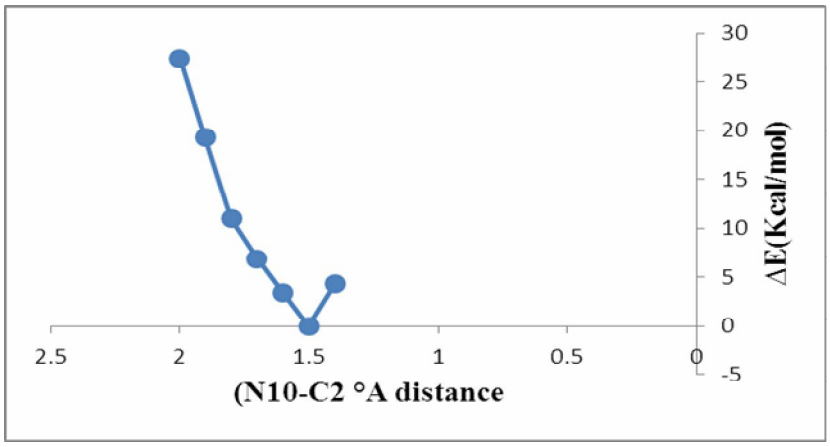


**Fig. 3.** The two dimensional scan of the obtained TS1 structure. Each point on this diagram is the performance of the probable state in this manner.

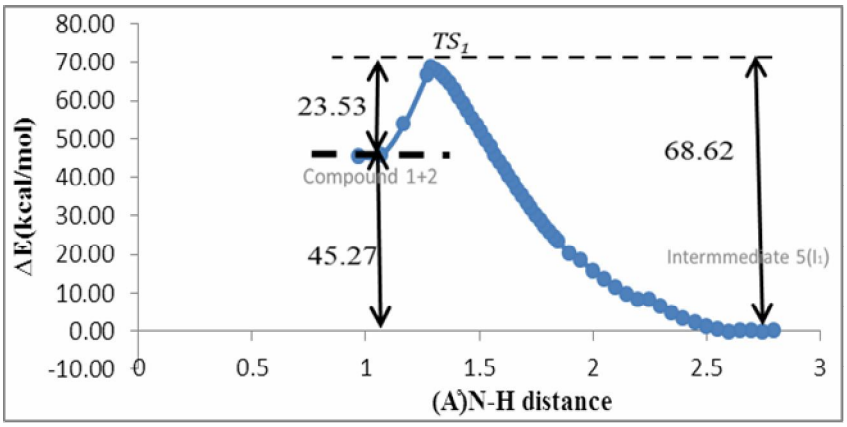


**Fig. 4.** The potential energy profile for $step_1$ of the proposed mechanism at the HF/6-311G(d,p) level.

at the HF/6-311G(d,p) level in the gas phase is 68.62 and 23.53 kcal $mol^{-1}$ higher than the energy of intermediate 5($I_1$) and compound 1+2, respectively (Fig. 4). Hence, this process is exothermic ($\Delta r$ = -45.27 kcal $mol^{-1}$) compared to the reactants. The energies of participating species in $step_1$ at both HF/6-311G(d,p) and B3LYP/6-311G(d,p) levels are shown in Table 2.

In the second step of this mechanism, two components of the reaction, aniline (3) and formaldehyde (4) react together.

The second step of the reaction occurs with the $N_{12}$-$C_{14}$ bond formation between aniline and formaldehyde for the generation of another intermediate 6($I_2$). Herein, $N_{12}$ is getting close to carbon $C_{14}$. For the generation of the $TS_2$ structure it was necessary to conduct the following procedure: we optimized B compound at the HF/6-311G(d, p) level and then in each step of scanning, the $N_{12}$-$C_{14}$ bond length is increased (0.1 Å), $H_{18}$ approaches to $N_{12}$ step by step until a peak is obtained (inverse two dimensional scanning). After each scan, the result was represented in a diagram. A same procedure with $step_1$ was employed for $step_2$, while the $N_{12}$-$C_{14}$ bond length was increased in each step (just 0.1 Å) of the process. The results are shown in Fig. 6.

**Table 2.** Energies of the Participating Species in $Step_1$ at Both HF/6-311G(d,p) and B3LYP/6-311G(d,p) Levels

| Step1 | B3LYP/6-311G(d,p) (kcal $mol^{-1}$) | HF/6-311G(d,p) (kcal $mol^{-1}$)[a] |
|---|---|---|
| Compound 1+2 | -515115.42 | -512051.54 |
| Ts | -515098.48 | -512028.07 |
| Intermediate 5($I_1$) | -515163.74 | -512102.43 |

In the second step of this mechanism, two components of the reaction, aniline (3) and formaldehyde (4) react together.

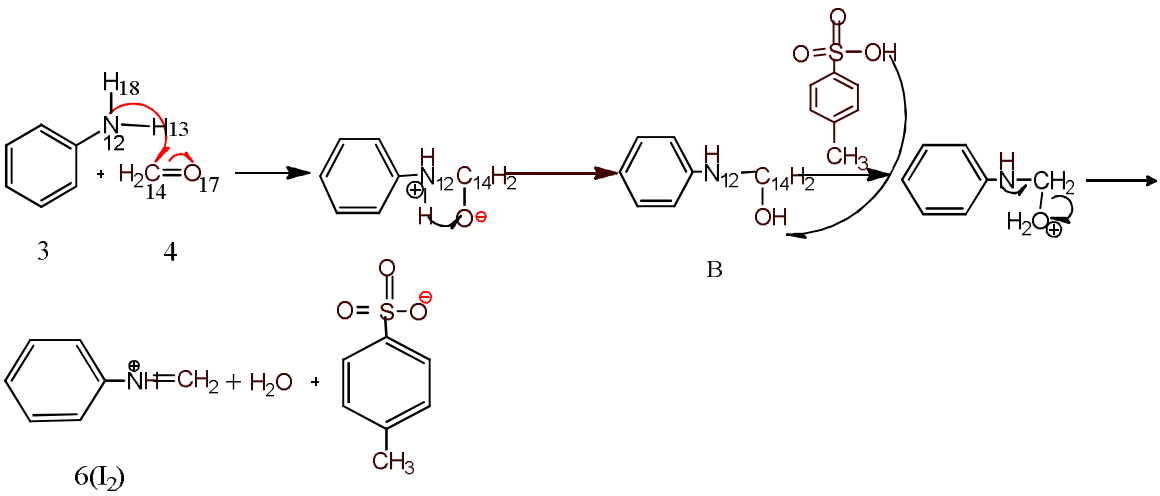


**Fig. 5.** $Step_2$ of the theoretical mechanism for the reaction between formaldehyde 4 and aniline 3 for the generation of intermediate 6($I_2$).

This diagram has a point with the lowest energy value that establishes the $TS_2$ structure (Fig. 6). The $TS_2$ energy at the HF/6-311G(d,p) level in the gas phase is 17.20 kcal $mol^{-1}$ which is 28.51 kcal $mol^{-1}$ higher than the energy of the stationary point compound (3+4) and intermediate 6($I_2$), respectively (Fig. 7). Hence, this process is exothermic ($\Delta r$ = -11.31 kcal $mol^{-1}$) compared to the reactants.

In the stationary point, the comparison of molecular geometries in reactants, $Ts_2$ and intermediate 6($I_2$) at HF/6-311G(d,p) level show that the $N_{12}$-C bond length changes from 1.38 to 1.43 and 1.39 Å, the $C_{14}$-$N_{12}$ bond length changes from 3.57 to 1.55, and 1.42 Å and $O_{17}$-$C_{14}$ from 1.2 to 1.39 and 1.43 Å, and the $O_{17}$-$C_{14}$-$N_{12}$ angles change from 60.61° to 94.47° and 114.55° and also the dihedral angle is 111.59° and 80.05° in the $TS_2$ and intermediate $I_2$. These changes are summarized in Table 3.

As can be seen, three significant changes would be prospect:

1) $N_{12}$-$C_3$ cleavage increase from reactant to $Ts_2$

2) $C_{14}$-$N_{12}$ bond length decrease in this order: intermediate 5 > $TS_2$ > compound 3+4

3) $C_3$-N-$C_{14}$ angles take significant increas from $TS_1$ to intermediate 6

The Energies of participating species in $step_2$ at the both

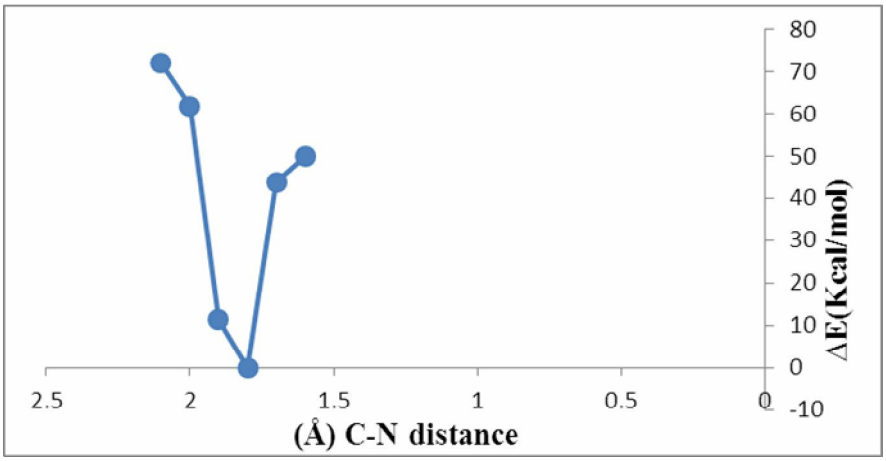


**Fig. 6.** The two dimensional scan of the obtained $TS_2$ structure.

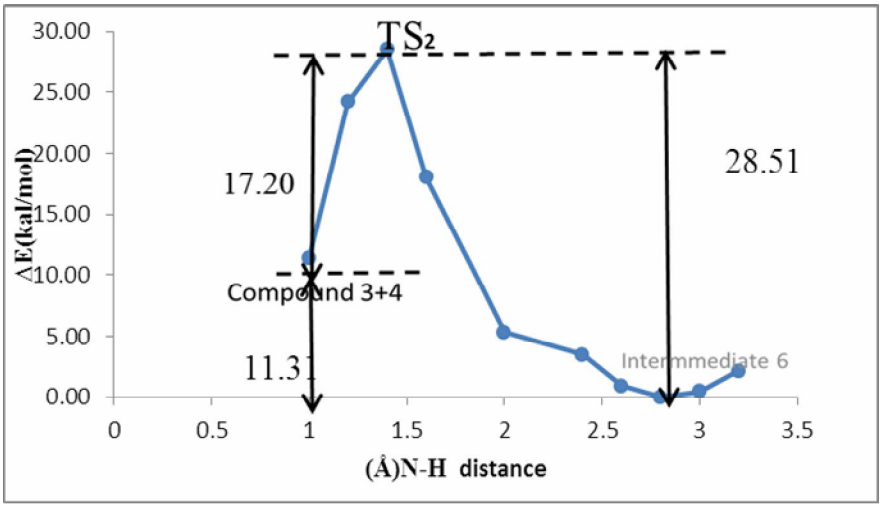


**Fig. 7.** The potential energy profile for $step_2$ of the proposed mechanism at the HF/6-311G(d,p) level.

HF/6-311G(d,p) and B3LYP/6-311G(d,p) levels are shown in Table 4.

The same procedure was employed for $step_3$, $step_4$ and $step_5$. All the relevant Figs. (1-7) and Tables (1-6) have been reported in the supplemental materials file (SMF). The first stretching frequencies for all steps of the mechanism at the HF/6-311G(d,p) and B3LYP/6-311G(d,p) levels of theory at 298.15 K are shown in Table 5 with respect to the sum of the result obtained from all the figures and tables mentioned in SMF. Activation parameters including $\Delta H^{\neq}$, $\Delta G^{\neq}$ and $\Delta S^{\neq}$ for each step of the speculative mechanisms at the HF/6-311G(d,p) and B3LYP/6-311G(d,p) levels at 298.15 K, are reported in Table 6.

As can be seen, the activation enthalpy ($\Delta H^{\neq}$) and the activation Gibbs free energy ($\Delta G^{\neq}$) for $step_2$ at higher level of theory (B3LYP/6-311G(d,p) are larger than the other steps which suggest that the energy required for $step_2$ is relatively high and it is an energetically unfavorable

**Table 3.** Some of the Bond Lengths, Bond Angles and Dihedral Angles of Step 2 of the Proposed Mechanism

| Species | Bond length (Å) | | | Bond angle (Degree) | | | Dihedral angle |
|---|---|---|---|---|---|---|---|
| | $N_{12}$-$C_3$ | $C_{14}$-$N_{12}$ | $O_{17}$-$C_{14}$ | $O_{17}$-$C_{14}$-$N_{12}$ | $H_{18}$-O-$C_{14}$- | $C_3$-N-$C_{14}$ | $O_{17}$-$C_{14}$-$N_{12}$-$C_3$ |
| Compound 3+4 | 1.38 | 3.57 | 1.2 | 60.61 | 109.12° | 109.68 | |
| $Ts_2$ | 1.43 | 1.55 | 1.39 | 94.47° | 76.19 | 119.88 | 115.59 |
| Intermediate 6 | 1.39 | 1.42 | 1.43 | 114.55 | 114.03 | 125.03 | 80.05 |

As can be seen, three significant changes would be prospect: 1) $N_{12}$-$C_3$ cleavage increase from reactant to $Ts_2$: 2) $C_{14}$-$N_{12}$ bond length decrease in this order: intermediate 5 > $TS_2$ > compound 3+4; 3) $C_3$-N-$C_{14}$ angles take significant increas from $TS_1$ to intermediate6

**Table 4.** Energies of Participating Species in Step 2 at the both HF/6-311G(d,p) and B3LYP/6-311G(d,p) Levels

| Step 2 | B3LYP/6-311G(d,p) (kcal $mol^{-1}$) | HF/6-311G(d,p) (kcal $mol^{-1}$)[a] |
|---|---|---|
| Compound 1+2 | -252400.96 | -250714.03 |
| Ts | -252408.55 | -250724.51 |
| Intermediate 5 | -252362.81 | -250667.65 |

process. Also the thermodynamic parameters including $\Delta_r H°$ (298.15 K), $\Delta_r G°$ (298.15 K) and $\Delta_r S°$ (298.15 K) calculated for each step, and also the overall reaction at HF/6-311G(d,p) and B3LYP/6-311G(d,p) at 298.15 K are presented in Tables 7 and 8, respectively.

In addition to the kinetic data including activation energies ($E_a$), the rate contestants ($k$) and pre-exponential factor (A) using Eyring Eq. (3) and Eq. (2) at the B3LYP/6-311g(d,p) and HF/6-311G(d,p) levels are reported in Tables 9 and 10, respectively. As can be seen, at both levels of the theory, $step_2$ is a rate determining step and $step_1$ is the fastest step. The $step_3$ is relatively fast, this is true, because in this step two intermediates, 5($I_1$) and 6($I_2$), react with each other. It seems that at higher level (B3LYP/6-311G(d,p)) the results are much more reliable than the HF/6-311G(d,p) level, because, step 3, which is a fast reaction between two intermediates 5($I_1$) and 6($I_2$), is kinetically more favorable at this level. Also the $step_5$ is relatively fast, because this step involves [1,3] hydrogen proton transfer which is usually fast process. The step 4, is relatively slow, because the five membered ring formation is inherently an energetically unfavorable process. Activation free Gibbs energy, as the rate constant, shows whether a step is fast or slow. Therefore, $step_3$ and $step_2$ have the maximum and minimum values of activation Gibbs free energy (Table 6) at both levels, respectively. Thus, $step_2$ and $step_3$ are the slow and fast steps, respectively. So, the second step is a rate-determining step which has Ea, forward = 45.90 kcal $mol^{-1}$ and $k_2 = 4.38 \times 10^{-25}$ (M $s^{-1}$) at the HF/6-311G(d,p) level (Table 10) and also Ea, forward = 36.92 kcal $mol^{-1}$ and $k_2 = 1.31 \times 10^{-17}$ (M $s^{-1}$) at B3LYP/6-311G(d,p) (Table 9).

**Table 5.** The First Stretching Frequency for all Steps of the Mechanism at HF/6-311G(d,p) and B3LYP/6-311G (d,p) Levels of Theory

| Species | First stretching frequency ($cm^{-1}$) | |
|---|---|---|
| | HF/6-311G(d,p) | B3LYP/6-311G(d,p) |
| Ground state of the reactants (1 and 2) in the step 1 | 23.3 | 23.6 |
| TS1 | 2138.7i | 1614.1i |
| Ground state of the product ($I_1$) in the step 1 | 25.2 | 20.2 |
| Ground state of reactants (3 and 4) in the step 2 | 20.7 | 27.3 |
| $TS_2$ | 1941.9i | 1620.1i |
| Ground state of the product ($I_2$) in the step 2 | 48.7 | 49.5 |
| Ground state of the reactants ( $I_1$ and $I_2$) in the step 3 | 14.1 | 12.2 |
| $TS_3$ | 400.5i | 144.1i |
| Ground state of the products ( $I_3$) in the step 3 | 16.5 | 5.3 |
| Ground state of the reactants ( $I_3$) in the step 4 | 11.9 | 17.2 |
| $TS_4$ | 1667.6i | 89.3i |
| Ground state of the products ( $I_4$) in the step 4 | 14.6 | 14.7 |
| Ground state of the reactants ( $I_4$) in the step 5 | 19.7 | 26.2 |
| $TS_5$ | 2396.0i | 2037.9i |
| Ground state of the final product in the step 5 | 19.8 | 23.9 |

$$Ea = \Delta H^{\ddagger}(T) + nRT \quad (1)$$

$$A = (ekBT/h)\exp(\Delta S\ddagger/R) \quad (2)$$

$$k = \frac{k_B T}{h} \times (R \times T)^{-\Delta n} \times e^{\frac{-\Delta H^{\mp}}{RT}} \times e^{\frac{\Delta S^{\mp}}{R}} \quad (3)$$

In addition, the overall thermodynamic reaction parameters for this mechanism are listed in Table 8. It was found that the reaction is thermodynamically favorable and spontaneous. The free Gibbs energy analysis shows that the mechanism is exothermic and values of $\Delta_r H°_{total}$ and $\Delta_r G°_{total}$ are large negative which implies that the reaction is exothermic and spontaneous and these features makes the reaction thermodynamically favorable. In addition the reaction is enthalpy controlled because the activation enthalpy ($\Delta H^{\neq}$) is much greater than $T\Delta S^{\neq}$ (Table 6).

## Kinetic Calculations

Based on the results presented, the simplified scheme for the proposed mechanism (Fig. 1) is shown in Fig. 8.

At first, the rate law is written using the final step for the formation of the product.

$$Rate = k_5[I_4] \quad (4)$$

**Table 6.** Activation Parameters ($\Delta G^{\ddagger}$ and $\Delta H^{\ddagger}$) and $\Delta S^{\ddagger}$, in kcal $mol^{-1}$, at 298.15 K, for each Step of the Mechanism for both Levels

| | | HF | B3LYP | | HF | B3LYP | | HF | B3LYP |
|---|---|---|---|---|---|---|---|---|---|
| $Step_1$ | $\Delta G^{\ddagger}_1$ | 19.333 | 10.35 | $\Delta H^{\ddagger}_1$ | 19.59 | 9.94 | $\Delta S^{\ddagger}_1$ | -0.86 | -1.37 |
| | $\Delta G^{\ddagger}_{-1}$ | 71.38 | 61.45 | $\Delta H^{\ddagger}_{-1}$ | 71.18 | 61.72 | $\Delta S^{\ddagger}_{-1}$ | 0. 67 | -9 |
| $Step_2$ | $\Delta G^{\ddagger}_2$ | 50.7 | 40.48 | $\Delta H^{\ddagger}_2$ | 45.31 | 36.32 | $\Delta S^{\ddagger}_2$ | -18 | -13.9 |
| $Step_3$ | $\Delta G^{\ddagger}_3$ | 19.3 | 7..94 | $\Delta H^{\ddagger}_3$ | 15.96 | 5.65 | $\Delta S^{\ddagger}_3$ | -10.6 | 7.6 |
| $Step_4$ | $\Delta G^{\ddagger}_4$ | 46.14 | 25.11 | $\Delta H^{\ddagger}_4$ | 44.43 | 22.55 | $\Delta S^{\ddagger}_4$ | 21.6 | 75.6 |
| $Step_5$ | $\Delta G^{\ddagger}_5$ | 42.56 | 23.48 | $\Delta H^{\ddagger}_5$ | 38.92 | 19.56 | $\Delta S^{\ddagger}_5$ | -12.2 | -13 |

**Table 7.** The Thermodynamic Parameters Includinh $\Delta_rH°$, $\Delta_rG°$ (kcal $mol^{-1}$) and $_{\Delta r}S°$ (cal $K^{-1}$ $mol^{-1}$) for each Step of the Mechanism at 298.15 K, at both Levels of the Theory

| Step | | HF | B3LYP | | HF | B3LYP | | HF | B3LYP |
|---|---|---|---|---|---|---|---|---|---|
| 1 | $\Delta_rH°_1$ | -51.58 | -51.78 | $\Delta_rG°_1$ | -52.043 | -51.1 | $\Delta_rS°_1$ | -1.53 | -2.3 |
| 2 | $\Delta_rH°_2$ | -8.283 | -5.517 | $\Delta_rG°_2$ | -3.419 | -1.854 | $\Delta_rS°_2$ | -16.3 | -12.3 |
| 3 | $\Delta_rH°_3$ | 0.1619 | -1.714 | $\Delta_rG°_3$ | 2.915 | 2.855 | $\Delta_rS°_3$ | -9.2 | -15.3 |
| 4 | $\Delta_rH°_4$ | 6.68 | 5.68 | $\Delta_rG°_4$ | 5.0195 | 4.344 | $\Delta_rS°_4$ | 6.1 | 4.5 |
| 5 | $\Delta_rH°_5$ | -7.605 | -6.344 | $\Delta_rG°_5$ | -3.018 | -7.735 | $\Delta_rS°_5$ | -26 | 4.6 |

**Table 8.** Overall Reaction Parameters Including $\Delta_rH°_{total}$, $\Delta_rG°_{total}$ and $\Delta_rS°_{total}$ at 298.15 K, at both Levels of the Theory

| $T\Delta S^{\neq}$ | $\Delta_rH°^{a}_{total}$ | | $\Delta_rG°^{a}_{total}$ | | $\Delta_rS°^{b}_{total}$ | |
|---|---|---|---|---|---|---|
| | HF | B3LYP | HF | B3LYP | HF | B3LYP |
| | -60.4 | -59.7 | -53.5 | -50.6 | -0.02 | -0.032 |

[a]kcal $mol^{-1}$. [b]cal $mol^{-1}$ $K^{-1}$.

**Table 9.** Rate Constant and Activation Energies for all Steps of the Mechanism at the B3LYP/6-311G(d,p) Level

| Step | Rate constant<br>Steps 1,2 and 3 ($mol^{-1}$ l $s^{-1}$)<br>Steps 4 and 5 ($s^{-1}$) | Pre-exponential factor (frequency factor)<br>($mol^{-1}$ l $s^{-1}$) | $E_a$ forward<br>(kcal $mol^{-1}$) |
|---|---|---|---|
| 1 | $k_1 = 1.5 \times 10^{5}$ | $A_1 = 8.46 \times 10^{10}$ | 10.54 |
| 2 | $k_2 = 1.3 \times 10^{-17}$ | $A_2 = 1.5 \times 10^{10}$ | 36.92 |
| 3 | $k_3 = 9.3 \times 10^{-6}$ | $A_3 = 3.5 \times 10^{11}$ | 6.25 |
| 4 | $k_4 = 2.4 \times 10^{-9}$ | $A_4 = 2.27 \times 10^{8}$ | 23.24 |
| 5 | $k_5 = 3.77 \times 10^{-5}$ | $A_5 = 2.62 \times 10^{10}$ | 20.15 |

**Table 10.** Rate Constant and Activation Energies for all Steps of the Mechanisms at HF/6-311G(d,p)

| Step | Rate constant<br>Steps 1,2 and 3 ($mol^{-1}$ l $s^{-1}$)<br>Steps 4 and 5 ($s^{-1}$) | Pre-exponential factor (frequency factor)<br>($mol^{-1}$ l $s^{-1}$) | $E_a$ forward<br>(kcal $mol^{-1}$) |
|---|---|---|---|
| 1 | $k_1 = 4.5 \times 10^{-2}$ | $A_1 = 2.6 \times 10^{13}$ | 20.19 |
| 2 | $k_2 = 4.38 \times 10^{-25}$ | $A_2 = 1.96 \times 10^{9}$ | 45.90 |
| 3 | $k_3 = 5.91 \times 10^{-2}$ | $A_3 = 8.07 \times 10^{10}$ | 16.55 |
| 4 | $k_4 = 4.42 \times 10^{-18}$ | $A_4 = 9.42 \times 10^{11}$ | 39.51 |
| 5 | $k_5 = 9.8 \times 10^{-16}$ | $A_5 = 3.6 \times 10^{10}$ | 36.37 |

We can apply the steady-state approximation to $[I_4]$, $[I_3]$, $[I_2]$ and $[I_1]$ .To obtain a suitable expression for $[I_4]$, $[I_3]$, $[I_2]$ and $[I_1]$, we can assume that after an initial brief period the concentration of $[I_4]$, $[I_3]$, $[I_2]$ and $[I_1]$ achieve a steady state while their rates of formation and disappearance are balanced. Therefore, $\frac{d[I_4]}{dt}$, $\frac{d[I_3]}{dt}$, $\frac{d[I_2]}{dt}$ and $\frac{d[I_1]}{dt}$ are zero and we can obtain expressions for the intermediates as follows:

$$\frac{d[I_4]}{dt} = k_4[I_3] - k_5[I_4] = 0$$

$$[I_4] = \frac{k_4[I_3]}{k_5} \quad (5)$$

$$\frac{d[I_3]}{dt} = k_3[I_2][I_1] - k_4[I_3] = 0, \quad [I_3] = \frac{k_3[I_2][I_1]}{k_4} \quad (6)$$

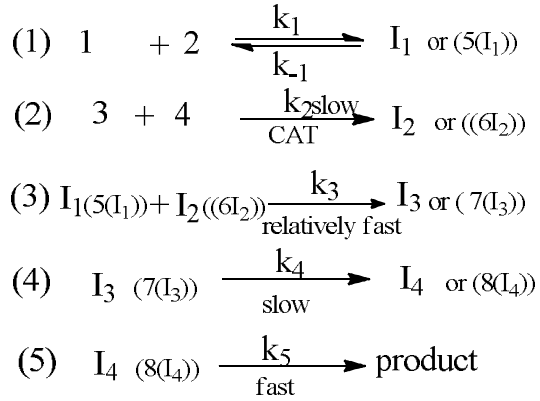


**Fig. 8.** A simplified proposed scheme for the reaction mechanism.

$$\frac{d[I_2]}{dt} = k_2[I_3][I_4] - k_3[I_2]\,[I_1] = 0\text{,}\quad [I_2] = \frac{k_2[3]\,[4]}{k_3[I_1]} \tag{7}$$

$$\frac{d[I_1]}{dt} = k_1[1][2] - k_{-1}[I_1] - k_3[I_1][I_2] = 0\text{,}\quad [I_1] = \frac{k_3[1]\,[2]}{k_{-1} + k_3[I_3]} \tag{8}$$

The value of (6) can be replaced in Eq. (5) to yield Eq. (9)

$$[I_4] = \frac{k_3[I_2]\,[I_1]}{k_5} \tag{9}$$

and with the replacement of Eqs. (7) and (8) in (9), the following equation is obtained:

$$[I_4] = \frac{k_2[3]\,[4]}{k_5} \tag{10}$$

With the replacement of Eqs. (10) in (4), the rate equation becomes:

$$\text{Rate} = k_2[3]\,[4] \tag{11}$$

The final equation indicates that the overall order of the reaction is two. In addition, according to this equation, partial orders with respect to each reactant of step 2, namely aniline (3) and formaldehyde (4), are 1 and 1, respectively. In addition, the rate constants such as $k_1$, $k_3$, $k_4$ and $k_5$ could not be seen in the rate law (11), so these steps are not rate determining steps. Step 2 is only the RDS and this is in agreement with the theoretical results.

## CONCLUSIONS

In this work, detailed kinetics and mechanism of the reaction between dimethyl acetylenedicarboxylate (DMAD) 2 and aniline 1 and formaldehyde 4 were theoretically studied in the presence of ρ-TsOH.$H_2O$ for the generation of mono-N-aryl-3-aminodihydropyrrol-2-one-4-carboxylates.

By considering the kinetic data and thermodynamic parameters of the mechanism, the following results can be asserted:

1. At both levels of theory, the second step of the mechanism (step 2) was recognized as a rate-determining step among the competition steps involved the reaction mechanism with Ea, forward = 45.90 kcal $mol^{-1}$ and $k_2$ = 4.38 × $10^{-25}$ (M $s^{-1}$) at HF/6-311G(d,p) and also *Ea*, forward = 36.2 kcal $mol^{-1}$ and $k_2$ = 1.31 × $10^{-17}$ (M $s^{-1}$) at B3LYP/6-311G(d,p) level of theory.
2. The third step ($step_3$) of the mechanism was recognized as a fast step with *Ea*, forward = 16.55 kcal $mol^{-1}$ and $k_3$ = 5.91 × $10^{-2}$ (M $s^{-1}$) at HF/6-311G(d,p) and *Ea*, forward = 6.25 kcal $mol^{-1}$ and $k_3$ = 9.3 × $10^{-6}$ (M $s^{-1}$) at B3LYP/6-311G(d,p). This is a logical fact because in this step both the intermediates $5(I_1)$ and $6(I_2)$ react together.
3. The $step_4$ is relatively slow because the five membered ring formation is inherently an energetically unfavorable process.
4. Also, $step_5$ is considerably fast because of the [1,3] H-shift which is usually a fast process.

5. $\Delta_rH°_{total}$ and $\Delta_rG°_{total}$ of the overall reaction were 59.6768 kcal $mol^{-1}$ and -50.54 kcal $mol^{-1}$, respectively, at B3LYP/6-311G(d,p) level, indicating that the reaction is exothermic and spontaneous process and it is thermodynamically favorable.

6. The theoretical kinetic studies show that the overall order of reaction is two, which is overall order of the reaction with respect to each reactant that participate in step 2 namely aniline (3) and formaldehyde (4).

7. The reaction is enthalpy-controlled because the value of ($\Delta H^{\neq}$) is much greater than $T\Delta S^{\neq}$.

8. Activation enthalpy ($\Delta H^{\neq}$) and Gibbs free energy ($\Delta G^{\neq}$) for $step_2$ at higher level (B3LYP/6-311G(d,p)) are larger than the other steps involved the reaction mechanism, suggesting that the reaction is chemically-controlled.

9. The results at higher level (B3LYP/6-311G(d,p)) were are in better agreement with the experimental results.

## ACKNOWLEDGEMENTS

We gratefully acknowledge financial support from the Research Council of the University of Sistan and Baluchestan.

## REFERENCES

[1] Dömling, A., Recent developments in isocyanides based multicomponent reactions in applied chemistry. *Chem. Rev.* **2006**, *106*, 17-89, DOI: 10.1021/cr0505728.

[2] Domling, A.; Ugi, I., Multicomponent reactions with isocyanides. *Angew. Chem. Int. Ed. Engl.* **2000**, *39*, 3168-3210, DOI: 10.1002/1521-3773.

[3] Zhu, J.; Bienaymé, H. (Eds.), Index, in Multicomponent Reactions, Wiley-VCH Verlag GmbH & Co. KGaA, Weinheim, FRG, 2005. DOI: 10.1002/3527605118.

[4] Souza, D.; Daniel M.; Mueller, Th., Multi-component syntheses of heterocycles by transition-metal catalysis. *Chem. Soc. Rev.* **2007**, *36*, 1095-1108, DOI: 10.1039/B608235C.

[5] Bellucci, M. C.; Volonterio, A., *Org. Chem. Insights.* **2012**, *4*, 1-24, DOI: org/10.1016/j.tetlet.2012.06.109.

[6] Zhu, J. J.; Bienaymé, H., Multicomponent reactions. John Wiley & Sons, 2006, DOI: 10.7536/PC140110.

[7] Selander, N., Development of Multi-Component Reactions using Catalytically Generated Allyl Metal Reagents," (Doctoral dissertation, Stockholms universitet), 2008.

[8] Eicher, T.; Hauptmann, S.; Speicher, A., Five-Membered Heterocycles: Sections 5.1-5.21. The Chemistry of Heterocycles: Structure, Reactions, Syntheses, and Applications, Second Edition, 2003, 52-121, DOI: 10.1002/352760183X.ch5a.

[9] Zhang, P. Z.; Zhou, S. F.; Li, T. R.; Jiang, L. Efficient synthesis and *in vitro* antifungal activity of 1H-benzimidazol-1-yl acetates/propionates containing 1H-1,2,4-triazole moiety. *Chinese Chem. Lett.,* **2012**, *23*, 1381-1384. DOI: 10.1016/J.cclet.2012.10.024.

[10] Akhaja,T. N.; Raval, J. P., Design, *Chin. Chem. Lett.* **2012**, *43*, 23446-449, DOI: 10.1002/chin.201212164.

[11] Bai, W. J.; Jackson, S. K.; Pettus, T. R., Mild construction of 3-methyl tetramic acids enabling a formal synthesis of palau'imide. *Org. Lett.,* **2012**, *14*, 3862-3865, DOI: 10.1021/ol301556a.

[12] Aginagalde, M.; Bello, T.; Masdeu, C.; Vara, Y.; Arrieta, A.; Cossío, F. P., Formation of γ-oxoacids and 1H-pyrrol-2(5H)-ones from α,β-unsaturated ketones and ethyl nitroacetate. *J. Org. Chem.,* **2010**, *75*, 7435-7438. DOI: 10.1021/jo101388x.

[13] Anaraki-Ardakani, H.; Noei, M.; Tabarzad, A., Facile synthesis of N-(arylsulfonyl)-4-ethoxy-5-oxo-2,5-dihydro-1H-pyrolle-2,3-dicarboxylates by one-pot three-component reaction. *Chinese Chem. Lett.*, **2012**, *23*, 45-48, DOI:10.1016/j.cclet.2011.09.010.

[14] Ettlinger, L.; Gäumann, E.; Hütter, R.; Keller-Schierlein, W.; Kradolfer, F.; Neipp, L.; Zähner, H.; Stoffwechselprodukte von actinomyceten 17. MitteilungHolomycin. *Helvetica Chim. Acta,* **1959**, *42*, 563-569, DOI: 10.1002/hlca.19590420225.

[15] Shiozawa, H.; Kagasaki, T.; Torikata, A.; Tanaka, N.; Fujimoto, K.; Hata, T.; Takahashi, S., Thiomarinols B and C, new antimicrobial antibiotics produced by a marine bacterium. *J. Antibiotics,* **1995**, *48*, 907-909. DOI: 10.7164/antibiotics.48.907.

[16] Singh, S. B.; Goetz, M. A.; Jones, E. T.; Bills, G. F.; Giacobbe, R. A.; Herranz, L.; Williams Jr, D. L., Oteromycin: a novel antagonist of endothelin

receptor. *J. Org. Chem*., **1995**, *60*, 7040-7042, DOI: 10.1021/jo00126a071.

[17] He, H.; Yang, H. Y.; Bigelis, R.; Solum, E. H.; Greenstein, M.; Carter, G. T., Pyrrocidines A and B, new antibiotics produced by a filamentous fungus. *Tetrahedron Lett.,* **2002**, *43*, 1633-1636. DOI: 10.1016/S0040-4039(02)00099-0.

[18] Clark, A. J.; Dell, C. P.; McDonagh, J. M.; Geden, J.; Mawdsley, P., Oxidative 5-endo cyclization of enamides mediated by ceric ammonium nitrate. *Org. lett.*, **2003**, *5*, 2063-2066. DOI: 10.1021/ol030045f.

[19] Chen, J.; Huang, P. Q.; Queneau, Y., Enantioselective synthesis of the R-enantiomer of the feeding deterrent (S)-Ypaoamide. *J. Org. Chem*. **2009**, *74*, 7457-7463. DOI: 10.1021/jo901557h.

[20] Raghuraman, A.; Ko, E.; Perez, L. M.; Ioerger, T. R.; Burgess, K., Pyrrolinone-pyrrolidine oligomers as universal peptidomimetics. *J. Am. Chem. Soc.,* **2011**, *133*, 12350-12353, DOI: 10.1021/ja2033734.

[21] Kawasuji, T.; Fuji, M.; Yoshinaga, T.; Sato, A.; Fujiwara, T.; Kiyama, R., 3-Hydroxy-1,5-dihydro-pyrrol-2-one derivatives as advanced inhibitors of HIV integrase. *Bioorg. Med. Chem.* **2007**, *15*, 5487-5492, DOI: 10.1016/J.bmc.2007.05.052.

[22] Zhang, L.; Tan, Y.; Wang, N. X.; Wu, Q. Y.; Xi, Z.; Yang, G. F., Design, syntheses and 3D-QSAR studies of novel N-phenyl pyrrolidin-2-ones and N-phenyl-1H-pyrrol-2-ones as protoporphyrinogen oxidase inhibitors. *Bioorg. Med. Chem*. **2010**, *18*, 7948-7956, DOI: 10.1016/J.bmc.2010.09.036.

[23] Mizushina, Y.; Kobayashi, S.; Kuramochi, K.; Nagata, S.; Sugawara, F.; Sakaguchi, K., Epolactaene, a novel neuritogenic compound in human neuroblastoma cells, selectively inhibits the activities of mammalian DNA polymerases and human DNA topoisomerase II. *Biochem. Biophys. Res. Commun*. **2000**, *273*, 784-788, DOI: 10.1006/bbrc.2000.3007.

[24] Zhu, Q.; Gao, L.; Chen, Z.; Zheng, S.; Shu, H.; Li, J.; Liu, S., A novel class of small-molecule caspase-3 inhibitors prepared by multicomponent reactions. *Eur. J. Med. Chem.* **2012**, *54*, 232-238, DOI: 10.1016/J.ejmech.2012.05.001.

[25] Li, B.; Lyle, M. P.; Chen, G.; Li, J.; Hu, K.; Tang, L.; Webster, J., Substituted 6-amino-4H-[1,2]dithiolo[4,3-b]pyrrol-5-ones: synthesis, structure–activity relationships, and cytotoxic activity on selected human cancer cell lines. *Bioorg. Med. Chem.* **2007**, *15*, 4601-4608. DOI: 10.1016/J.bmc.2007.04.017.

[26] Demir, A. S.; Aydogan, F.; Akhmedov, I. M., The synthesis of chiral 5-methylene pyrrol-2(5H)-ones *via* photooxygenation of homochiral 2-methylpyrrole derivatives. *Tetrahedron: Asymmetr.* **2002**, *13*, 601-605. DOI: 10.1016/S0957-4166(02)00140-4.

[27] Reddy, T. R.; Li, C.; Guo, X.; Myrvang, H. K.; Fischer, P. M.; Dekker, L. V., Design, synthesis, and structure-activity relationship exploration of 1-substituted 4-aroyl-3-hydroxy-5-phenyl-1H-pyrrol-2 (5H)-one analogues as inhibitors of the annexin A2-S100A10 protein interaction. *J. Med. Chem.* **2011**, *54*, 2080-2094, DOI: 10.1021/jm101212e.

[28] Shahraki, M.; Habibi-Khorassani, S. M.; Dehdab, M., Effect of different substituents on the one-pot formation of 3,4,5-substituted furan-2(5H)-ones: a kinetics and mechanism study. *RSC Adv.* **2015**, *5*, 52508-52515. DOI: 10.1039/C5RA09717.

[29] Khorassani, S. M. H.; Ebrahimi, A.; Maghsoodlou, M. T.; Shahraki, M.; Price, D., Establishing a new conductance stopped-flow apparatus to investigate the initial fast step of reaction between 1,1,1-trichloro-3-methyl-3-phospholene and methanol under a dry inert atmosphere. *Analyst,* **2011**, *136*, 1713-1721. DOI: 10.1039/C0AN00817F.

[30] Shahraki, M.; Habibi-Khorassani, S. M., Kinetic spectrophotometric approach to the reaction mechanism of pyrrole phosphorus ylide formation based on monitoring the zwitterionic intermediate by using the stopped-flow technique. *J. Phys. Org. Chem.* **2015**, *28*, 396-402, DOI: 10.1002/poc.3424.

[31] Pourpanah, Sh.; Habibi-Khorassani, S. M.; Shahraki, M., Kinetic study of the reaction of 2-aminobenzamid with 2,6-dicholorobenzald-ehyde for producing 2-(2,6-dichlorophenyl)-2,3-dihydroquinazolin-4(1H)-one, *Chinese J. Catal.* **2015**, *36*, 757-763, DOI: https://doi.org/10.1016/S1872-2067(14)60302-8.

[32] Shaharaki, M.; Habibi-Khorassani, S. M., Kinetic aspects of tetrahydrobenzo[b]pyran formation in the presence of agar as a green catalyst: A mechanistic investigation, *Biosci. Biotech. Res. Asia,* **2016**, *13*,

715-723. DOI: 10.13005/bbra/2090.

[33] Shahraki, M.; Habibi-Khorassani, S. M.; Ebrahimi, A.; Maghsoodlou, M.; Ghalandarzehi, Y., Intramolecular hydrogen bonding in chemoselective synthesized 2-substituted pyrrole stable phosphorus ylide: GIAO, AIM, and NBO approaches. *Struct Chem*. **2013**, *24*, 623-635. DOI: 10.1007/s11224-012-0114-z.

[34] Dehdab, M.; Habibi-Khorassani, S. M.; Shahraki, M., Kinetics and mechanism investigation of the synthesized highly diasteroselective substituted tetrahydropyridines in the presence of la (no3) 3.6 h2o as a catalyst. *Catal lett,* **2014**, *144*, 1790-1796, DOI: 10.1007/s10562-014-1338-x.

[35] Habibi-Khorassani, S. M.; Maghsoodlou, M. T.; Shahraki, M.; Poorshamsoddin, M. A.; Karima, M.; Abbasi, M., Sucrose catalyzes synthesis of 2-amino-4H-chromene: Insight to the kinetics, *Iran. J. Catal.,* **2015**, *5*, 79-87.

[36] Darijani, M.; Habibi□Khorassani, S. M.; Shahraki, M., A Thermodynamic and Kinetic Insight into the Pathways Leading to a Highly Functionalized Ketenimine: A Computational Study. *Int. J. Chem. Kinet.,* **2015**, *47*, 751-763, DOI: 10.1002/kin.20946.

[37] Ghasemi, K.; Rezvani, A. R.; Habibi-Khorassani, S. M.; Shahraki, M.; Shokrollahi, A.; Moghimi, A.; Gavahi, S., An experimental and theoretical study of a hydrogen-bonded complex: *O*-phenylenediamine with 2, 6-pyridinedicarboxylic acid. *J. Mol. Struct.* **2015**, *1100*, 597-604, DOI: 10.1016/J.molstruc.2015.07.077.

[38] Habibi-Khorassani, S. M.; Shahraki, M.; Maghsoodlou, M. T.; Erfani, S., Dynamic $^{1}$H NMR studies of hindered internal rotations in the synthesized particular phosphorus ylide: Experimental and theoretical approaches. *Spectrochim. Acta Part A.* **2015**, *145*, 410-416. DOI:10.1016/j.saa.2015.02.084.

[39] Sajadikhah, S. S.; Maghsoodlou, M. T.; Hazeri, N., A simple and efficient approach to one-pot synthesis of mono-and bis-N-aryl-3-aminodihydropyrrol-2-one-4-carboxylates catalyzed by InCl 3. *Chinese Chem. Lett.* **2014**, *25*, 58-60, DOI: 10.1016/J.CCLET. 2013.10.010.

[40] Petersson, A.; Bennett, A.; Tensfeldt, T. G.; Al-Laham, M. A.; Shirley, W. A.; Antzaris, J., A complete basis set model chemistry. I. The total energies of closed-shell atoms and hydrides of the first-row elements. *J. Chem. Phys.* **1988**, *89*, 2193-2218. DOI: 10.1063/1.455064.

[41] Becke, A., D Density-functional exchange-energy approximation with correct asymptotic behavior. *Phys. Rev. A,* **1988**, *38*, 3098. DOI: 10.1103/ physRevA.38.3098.

[42] Frisch, M. J.; Trucks, G. W.; Schlegel, H. B.; Scuseria, G. E.; Robb, M. A.; Cheeseman, J. R.; Scalmani, G.; Barone,V.; Mennucci, B.; Petersson, G. A.; Nakatsuji, H.; Caricato, M.; Li, X.; Hratchian, H. P.; Izmaylov, A. F.; Bloino, J.; Zheng, G.; Sonnenberg, J. L.; Hada, M.; Ehara, M.; Toyota, K.; Fukuda, R.; Hasegawa, J.; Ishida, M.; Nakajima, T.; Honda, Y.; Kitao, O.; Nakai, H.; Vreven, T.; Montgomery, J. A.; Jr., Peralta, J. E.; Ogliaro, F.; Bearpark, M.; Heyd, J. J.; Brothers, E.; Kudin, K. N.; Staroverov, V. N.; Kobayashi, R.; Normand, J.; Raghavachari, K.; Rendell, A.; Burant, J. C.; Iyengar S. S.; Tomasi, J.; Cossi, M.; Rega, N.; Millam, J. M.; Klene, M.; Knox, J. E.; Cross, J. B.; Bakken, V.; Adamo, C.; Jaramillo, J.; Gomperts, R.; Stratmann, R. E.; Yazyev, O.; Austin, A. J.; Cammi, R.; Pomelli, C.; Ochterski, J. W.; Martin, R. L.; Morokuma, K.; Zakrzewski, V. G.; Voth, G. A.; Salvador, P.; Dannenberg, J. J.; Dapprich, S.; Daniels, A. D.; Farkas, O.; Foresman, J. B.; Ortiz, J. V.; Cioslowski, J.; and Fox, D. J.; Gaussian 09 Revision A. 1, 2009. Gaussian Inc. Wallingford CT.